Texture and electrical dynamics of micrometer and submicrometer bridges in misaligned $Tl_2Ba_2CaCu_2O_8$ films

J. Scherbel,[1] M. Mans,[1] H. Schneidewind,[2] U. Kaiser,[1] J. Biskupek,[1] F. Schmidl,[1] and P. Seidel[1]
[1]*Institut für Festkörperphysik, Friedrich-Schiller-Universität Jena, D-07743 Jena, Germany*
[2]*Institut für Physikalische Hochtechnologie e.V., Albert-Einstein-Str. 9, D-07745 Jena, Germany*
(Received 25 February 2004; published 16 September 2004)

Different thin $Tl_2Ba_2CaCu_2O_8$ layers were grown on 20° vicinal cut $LaAlO_3$ substrates by means of a two-step process. SEM pictures showed that thin film layers with a thickness smaller than 150 nm grow completely in the 20° misalignment given by the substrate but they also show few holes in the films. Thicker layers showed areas of *c*-axis growth beneath the expected misaligned texture whereas the allotment and numbers of *c*-axis islands depend on the layer thickness. TEM investigations in the selected area of misaligned growth showed a clear epitaxial relationship between the substrate and the film but they also revealed a domain like growth of the layers with plain $Tl_2Ba_2CaCu_2O_8$ grains and stacking faults. Furthermore, the films had a rather high surface roughness depending on the layer thickness. Thin films with a thickness of 120 nm were used to pattern micro- and sub-micrometer bridges. Because of the misaligned growth and the high anisotropy of the $Tl_2Ba_2CaCu_2O_8$ the bridges formed serial arrays of intrinsic Josephson junctions. Electrical measurements on these bridges revealed very complex dynamics within such devices. The current-voltage characteristics showed the well known branch structure of intrinsic Josephson junction arrays but with a statistical distribution of the transition currents from measurement to measurement. The temperature dependencies of the smallest critical currents generally deviated from the Ambegaokar-Baratoff theory. There was no complete suppression of the super current in an effective B-field up to 4.2 T. The analysis of the current-voltage characteristics indicated a collective transition switching especially in the first few transitions. Those could be split up by the application of a magnetic field and by the irradiation of mm-waves but not by an increment of the operation temperature. Furthermore, distinct two level fluctuations and chaotic like behavior were observed.

DOI: 10.1103/PhysRevB.70.104507 PACS number(s): 74.72.Jt, 07.57.Hm, 74.50.+r, 74.81.Fa, 74.40.+k

I. INTRODUCTION

Some high-temperature superconductor (HTS) ceramics have a strong anisotropy in its lattice. This leads to intrinsic Josephson effects for *c*-axis transport currents which were firstly discovered on small stacks of $Bi_2Sr_2CaCu_2O_8$ single crystals.[1] A finite thickness of some nanometers along the *c*-axis of this material already offers the possibility to create a serial array of many Josephson junctions with a high package density. In these ceramics the coherence length of Copper pairs along the *c*-axis is often much shorter than the spacing between the superconducting Cu-O planes. This leads to rather high characteristic voltages. Therefore, the Josephson current in the intrinsic junctions can oscillate within the sub-THz to lower THz range. Applications as sub-mm wave oscillators are promising and the RF emission of intrinsic Josephson junction stacks of several anisotropic HTSL single crystals have been investigated.[2] The preparation of stacks out of single crystals is quite difficult. Therefore the successful preparation of $Bi_2Sr_2CaCu_2O_8$[3] and of $Tl_2Ba_2Ca_2Cu_3O_8$[4] or of $Tl_2Ba_2CaCu_2O_8$ layers[5] were welcome. However, the thin film preparation of mesa-shaped stacks requires normal conducting top electrodes. To prevent a high contact resistance due to the interface between the normal conductor and the superconducting top layer of the mesas circumstantial technologies are necessary, too.[6–8] Furthermore the quasiparticle injection through the normal contacting electrode into the mesa leads to a quasiparticle underground in the current-voltage characteristics, distinct low-frequency noise due to two-level fluctuations[9] and to charge imbalance effects[10] which hobble the applicability of such devices. For whisker structures complete superconducting electrodes are possible. The double sided etching[11] is only practicable for single crystals, but the focused ion beam preparation[12] can be used for thin films, too. But in any case these technologies are difficult again. Several years ago Tsai *et al.* investigated few-micrometer wide strips of a $Bi_2Sr_2CaCu_2O_x$ thin film which *c*-axis was 4° misaligned from the substrate normal due to the respective orientation of the used $SrTiO_3$ substrate.[13] They found marked anisotropies in the two in plane transport orientations. Substrates suitable for RF applications are necessary such ones as, e.g., $LaAlO_3$. Later Chana *et al.* investigated microbidges of a 20° misaligned $Tl_2Ba_2CaCu_2O_8$ film on $LaAlO_3$.[14] The patterned microbridges clearly showed branch structures in the current-voltage characteristics which indicate intrinsic Josephson effects.[14–16] A BaCaCuO precursor was patterned for preparation firstly and oxy-thallinized subsequently. Warburton *et al.*[17] performed first investigations on complete grown 20° misaligned $Tl_2Ba_2CaCu_2O_8$ thin films. The advantages of the misaligned films are obvious: The planar patterning facilitates planar RF feed-back structures such as resonators, which are helpful for a synchronization of the single Josephson junctions in the array,[18–22] or tuning elements for a better RF matching as well as antenna structures for in- and out coupling of mm and sub-mm waves. Furthermore, superconducting bias feeds are naturally given. In this work we investigate the texture of different thin complete 20° misaligned $Tl_2Ba_2CaCu_2O_8$ films and the electronic features of different wide bridges of the prepared film with the lowest thickness. The measurement data show many interesting effects which can be put down to the texture of the investigated films mainly. Section II gives a short survey of the sample fabrication as well as some important information about the measurement setup. In Sec. III we describe the investigated epitaxy of complete $Tl_2Ba_2CaCu_2O_8$ layers with a 20° misalignment on a vicinal cut $LaAlO_3$ by scanning electron microscopy (SEM) as well as by transmission electron microscopy (TEM) and by atomic force microscopy (AFM) examinations on special samples. Section IV shows the results of the electrical characterization of micro- and submicrometer bridges patterned on a thin misaligned $Tl_2Ba_2CaCu_2O_8$ film. The results include the current-voltage characteristics at low temperatures, the statistical behaviour as well as the response to mm-wave irradiation and the magnetic field influence in selected cases, experiences from temperature as well as time dependent measurements. A summary and outlook can be found in Sec. V. We are convinced that this work gives a good overview on several interesting effects in the dynamics of misaligned stacks of intrinsic Josephson junctions which are worth to be investigated more separately and systematically in future.

II. FABRICATION AND MEASUREMENT SETUPS

The $Tl_2Ba_2CaCu_2O_8$ films were grown epitaxially on 20°-vicinal $LaAlO_3$ in a two step process. At first a Tl-free precursor of amorphous Ba-Ca-Cu-O was produced by RF-magnetron-sputtering. In a second step this precursor was oxy-thallinized in a thallium oxide atmosphere at high temperatures. A former publication[5] describes the details of this process. Films with thicknesses of 120 to 190 nm were prepared, for electrical characterizations the averaged film thickness was 120 nm. Photo lithographical techniques and Ar^+-ion beam milling were applied to pattern microbridges. A hole defect in the $Tl_2Ba_2CaCu_2O_8$ film offered the possibility for an exploration of a submicron bridge. Hence, micro bridges of 10 μm length and a width of 10 and 2 μm, respectively, and a 2 μm wide bridge with several constrictions so that its effective width reaches from 0.6 to 1.5 μm were electrical characterized. In the case of an ideal growth of the $Tl_2Ba_2CaCu_2O_8$ film and considering the unit cell dimensions and the 20° misalignment the 10 μm long bridges are supposed to contain about 1500 Josephson junctions in series.[14] The electrical measurements of the IV branches, the statistics of the switching current $I_S, I_S(T)$ and the time dependent measurements were arranged in a four-probe geometry. The microwave measurements and the studies in the magnetic field could be arranged in a two-probe geometry only. The several wires were shielded by grounded covers. The current bias and the voltage measurements were done by a low noise source and by a measurement unit from Keithley for averaged measurements and by a digital storage oscilloscope from Tektronix for time resolved measurements. The measurements were performed either in liquid Helium, in a flow through cryostat with integrated Niobium coil, which can supply a magnetic field of 5 Tesla or in a flow through cryostat with a window for microwave input, respectively. The RF irradiation of 93 GHz was supplied by a gun diode connected with a tunable attenuator and a horn antenna. A MgO lense was glued on the sample for the RF response measurements directly. Because the arrays of intrinsic Josephson junctions show a strong tendency to a statistical behavior we measured each IV characteristic up to 10 times for one current range as well as we measured 10 to 15 different current ranges for the record of a complete branch characteristic. In order to analyze the lower I_S-values we took 100 to 130 measurements. To allow the record of the hysteretic behavior all characteristics were measured in a bidirectional way. Furthermore we prepared cross-sectional samples for the TEM examination from a 180 nm thick film of $Tl_2Ba_2CaCu_2O_8$ on 20°-vicinal cut $LaAlO_3$. We used mechanical polishing, dimpling and low-angle Ar^+-ion milling. Microscopy was carried out by using a JEOL 3010 TEM, equipped with a LaB_6 cathode which operates at 300 kV. To prevent damages due to contamination processes we took the SEM images of several film surfaces with an acceleration voltage of 5 kV. The AFM examination was performed on the constricted microbridge only.

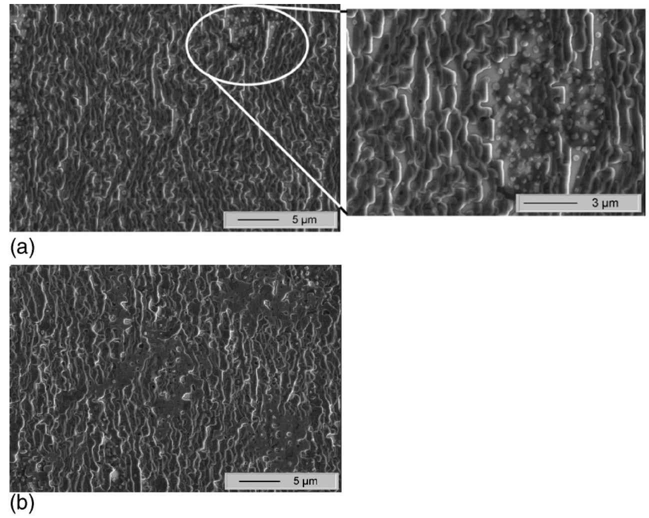

FIG. 1. SEM pictures of different thick $Tl_2Ba_2CaCu_2O_8$ layers grown on 20° misaligned $LaAlO_3$ {(a)–120 nm and (b)–190 nm}.

III. MICROSCOPY

A. SEM

SEM pictures of the $Tl_2Ba_2CaCu_2O_8$ surfaces show creased terrace structures which indicate the 20° misaligned *c*-axis growth of the layers. Furthermore the picture of the 120 nm thick film shows gaps in the terrace structure [Fig. 1(a)]. Thicker films do not show these gaps, but for thicknesses of 150 nm and above island shaped plateaus can bee seen [Fig. 1(b)]. These islands contain epitaxial $Tl_2Ba_2CaCu_2O_8$ where their *c*-axis points along the surface normal. The allotment and numbers of these islands depend on the layer thickness.

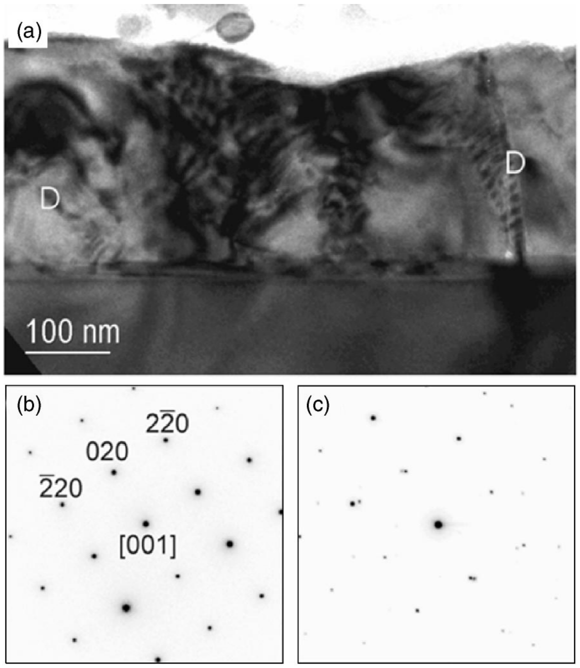

FIG. 2. Bright-field cross-section TEM scan of a 180 nm thick $Tl_2Ba_2CaCu_2O_8$ layer grown on 20° misaligned $LaAlO_3$ (a), with selected area diffraction patterns of substrate (b) and substrate together with the layer (c).

B. TEM

TEM cross-sectional investigations allow an insight into the structure along the growth direction however on a much smaller scale. The layer thickness and roughness at the depicted area can be evaluated easily. Bright-field studies at [001] orientation of the substrate [see, e.g., in Fig. 2(a)] showed that it varies between 300 and 150 nm with a grain size of about 500 nm up to 1 μm. The grains are single crystalline and separated by defects (marked D) as stacking faults and grain boundaries. The large surface roughness as depicted in SEM and AFM (below) can also be seen in TEM images. Selected area diffraction patterns from substrate only [Fig. 2(b)] and from a region including layer and substrate [Fig. 2(c)] revealed that the layer is grown epitaxially on the substrate with the orientation relationship $[001]_{\mathrm{substrate}}$ parallel $[001]_{\mathrm{layer}}$ and $[-220]_{\mathrm{substrate}}$ very close to $[-220]_{\mathrm{layer}}$, however a small missorientation can be seen (see also Fig. 3). Twin boundaries of the $LaAlO_3$ complicated the alignment of the electron beam basing on the substrate. This orientation twinning in the substrate is responsible for the creases in the terrace structures clearly visible in the SEM pictures. Otherwise we find that stacking faults of the substrate continued into the film rather seldom. This indicates a certain extent of a self determined growth of the film. The growth seems to be partly decoupled from the substrate information because the film tends to change its growth mode from tilted growth to an ordinary c-axis mode with parallel CuO planes at higher thickness [Fig. 1(b)].

C. AFM

Figure 4 shows the AFM record of the bridge with strong variation in widths. We measured a root-mean-square roughness from 12 to 14 nm, but maximum-minimum values up to 120 nm only for the film whereas outgrowths where unconsidered. These outgrowths reach elevations up to 1 μm. A lot of regions of the film show lowered areas. Some of these dents reach the dimension of holes (see Fig. 4 line A) as it can be seen in the SEM images for thin films too. Line B shows the constriction of 900 nm width and 120 nm height and it also shows the blind alley of about 500 nm width and 40 nm height. The elevations are composed of $Tl_2Ba_2CaCu_2O_8$. The area between them is lowered down to the ground level of the $LaAlO_3$ substrate. The tightest part of the bridge which allows a current flow was found in line C of the figure and it has a width of 600 nm and a height of 100 nm. In this region we presume the junctions with the smallest I_S values. The very complex shape of the borderline of the bridge proves that the origin of the constricting defects is located in the film structure itself and not in the patterning process. Nevertheless, this bridge was found to be the bridge with the highest stability and reproducibility in the electrical measurements (see below). It was superior to the wider bridges with more accurate border lines.

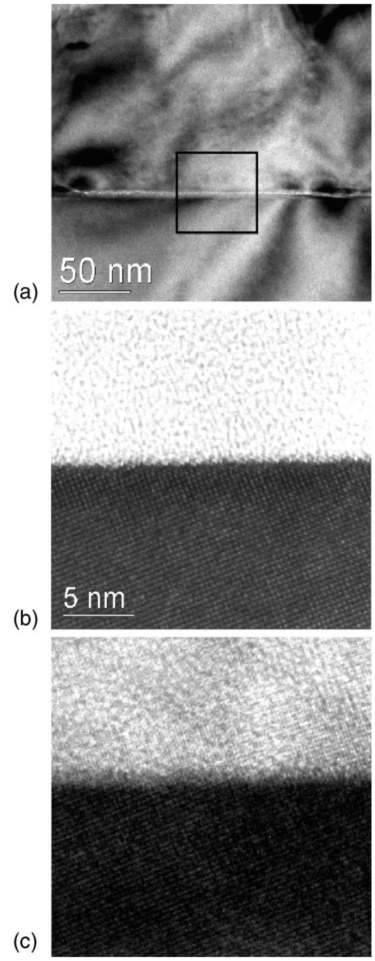

FIG. 3. (a) Close up from an area of Fig. 2(a). [(b) and (c)] High-resolution scan taken from the area marked in (a). In (b) the substrate and in (c) the layer are on zone axis conditions, indicating a small tilt in growth direction between layer and substrate.

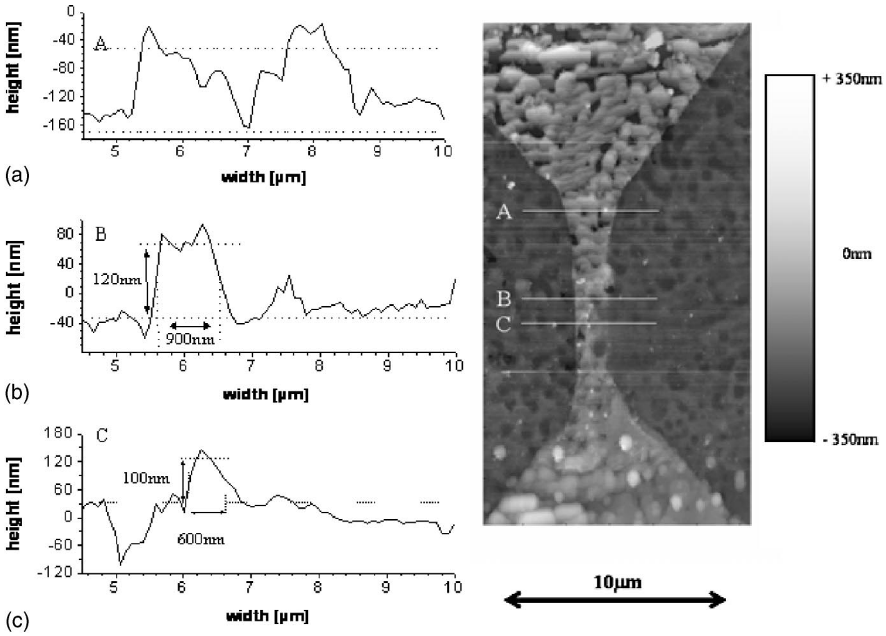

FIG. 4. AFM record of the constricted bridge. The lines in the right picture mark the respective height contour measurements shown on the left side.

IV. ELECTRICAL CHARACTERIZATIONS

A. IV branches

Figure 5 shows the IV characteristics of a constricted bridge with a width of 2 and 10 μm at 4.2 K. Note that these characteristics include 130–150 measurements in one graph. The bidirectional measurements of the IV curves yield the typical characteristics of intrinsic Josephson junctions with multiple branching. The different bridges show characteristics with very different properties, in particular concerning their stability. For the constricted bridge we find clearly separable branches. The 10 junctions (in rare cases 12 junctions) with the smallest switch current I_S of approximately 3.8 μA switch in a collective branch from the superconducting into the resistive state. We assume that the collective branch is not only caused by the switching of the same number of junctions but by the switching of the same junctions. A strong clue for this fact is the exact reproducibility of the common branch. The common branches will vary from each other if for several measurements the same number but different junctions with slightly different parameters switch into the resistive state. The next 10 branches show the individual switches of the Josephson junctions at I_S values from 4 μA to 12 μA. The typical values of the normal resistances R_N range from 2 to 3 kΩ, the values of the critical voltage jump V_C range from 14 to 18 mV. The characteristic of the 2 μm wide bridge shows a noticeable worse stability. The single branches are not clearly separable in a bundle of repeated measurements but they differ slightly. This indicates either the fact that the junctions did not switch everytime in the same sequence or that the biased current found different paths along the microbridge. The switching in different sequences is enabled by the statistical transition behavior of the junctions in such stacks which is represented below in this section. Otherwise the assumption of different current paths is potential due to the given texture of the $Tl_2Ba_2CaCu_2O_8$ film on the 20° misaligned $LaAlO_3$ substrate as it was pointed out in Sec. III. Furthermore, the first 8 junctions switch individually or in groups of up to 4 junctions at I_S values from 6 to 24 μA. The downward curves are trackable. However, for the next 5 or 6 junctions with I_S values from 23 to 28 μA a tracking of the downward curve is impossible because the switching of one of the next 6 or 7 junction branches is hardly avoidable. This indicates a rather good reproducible collective switching of a cluster of junctions in this stack. The next junctions show I_S values from 28 to 30 μA and trackable downward curves again. Typical R_N values reach from 1 to 2 kΩ and V_C from 15 to 20 mV. For the 10 μm wide bridge we found up to 40 branches with

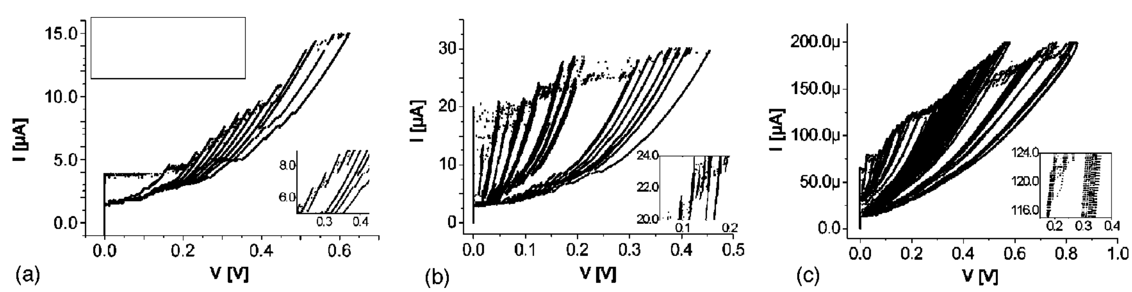

FIG. 5. The superposition of all measured IV characteristics of the constricted (a), the 2 μm wide (b) and the 10 μm wide bridge (c) at 4.2 K. The insets show a zoomed view into selected branch regions of the respective IV characteristics.

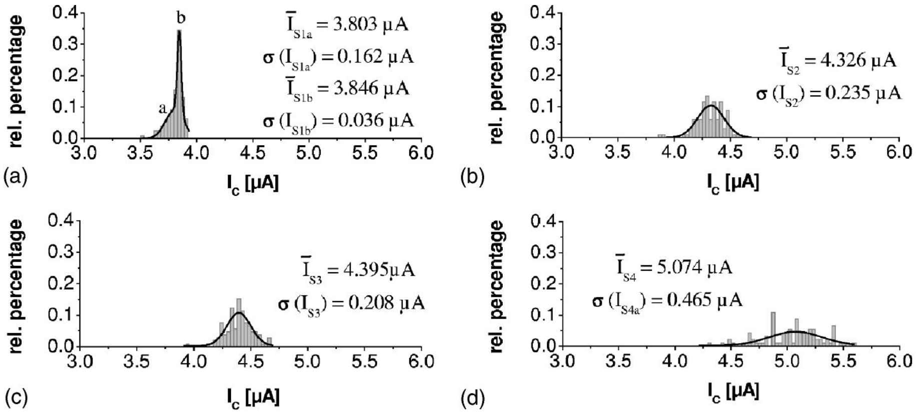

FIG. 6. The statistics of the four smallest transition current of the constricted microbridge at 4.2 K [first (a)–fourth (d)].

large difficulties to distinguish the several branches in the bundle of measurements. The I_S values range from 40 to 200 μA, R_N values reach some hundred Ohms and V_C range from 14 to 20 mV. Below 150 μA we found 15 individually switches and above 150 μA collective switches of 4 to 10 junctions. It is very remarkable that the current I_B, at which the junction stack switches back to the superconducting state, is not fixed but ranges from 17 to 30 μA.

B. Statistical behavior

1. General features

Because reproducible branches can be observed at the constricted bridge only we solely investigated the statistical behavior of the switching currents of Josephson junctions in this bridge. The measurements on the wider bridges present similar statistics but an allocation of the events is too difficult in these cases. We analyzed the I_S statistics of the junctions in the constricted bridge at 4.2 K which generates the first four branches in the IV characteristics. Figure 6 shows the acquired relative percentage diagrammed in histograms with column widths of 0.03 μA. The I_S distributions can be fitted by Gauss functions. For the distribution of the lowest switching current I_{S1} we have to fit with a double Gauss function. For the other distributions single Gauss peaks yield a good approximation. The values of the respective mean switching current I_{Sx} and the respective standard deviation $\sigma(I_{Sx})$ are noted in the figures. A more detailed analysis of the I_S distributions yield the fact that the first peak in the I_{S1} distribution is originated by slower measurements of the IV curves, the second one by faster measurements. The I_{S2}, I_{S3}, and I_{S4} statistics are nonsensitive for variations of the measurement speed. Furthermore it is obvious that the standard deviation of I_{S4} is larger than the ones of I_{S2} and I_{S3} which are quite similar. But all three standard deviations are substantial larger then $\sigma(I_{S1})$. A proper analysis of the respective jumps leads to the conclusion that the distribution of the switching currents depends on the number of junctions which switch together. So the first switching current I_{S1} is 129 times given by 10 junctions and once by 12 ones. I_{S2} is 95 times given by two junctions and 21 times by three ones. For I_{S3} 70 times one junction and 35 times three junctions are involved and I_{S4} is generated 91 times by a single junction and only once by two junctions. It seems that the junctions which switch together interact with each other so that the transition current distribution narrows. The determination of I_{S1} at different operating temperatures (Fig. 7) reveals that for higher temperatures there is no measurement velocity effect anymore because at a distinct temperature only a single peak in the distribution can be seen. Furthermore, a slight widening of the I_{S1} main distribution (peak b) at higher temperatures is obvious. This differs from the measurements from Mros *et al.* on long $Bi_2Sr_2CaCu_2O_{8-\delta}$ single crystal stacks[23] and Warburton on 2 μm$\times$2 μm microbridges of similar misaligned $Tl_2Ba_2CaCu_2O_8$ films.[17] Note, that the lateral geometries as well as the determination method of both groups are different from our ones.

2. Cause considerations

Mros *et al.* explained the origin of the switching current distribution by different quasi-equilibrium Josephson fluxon

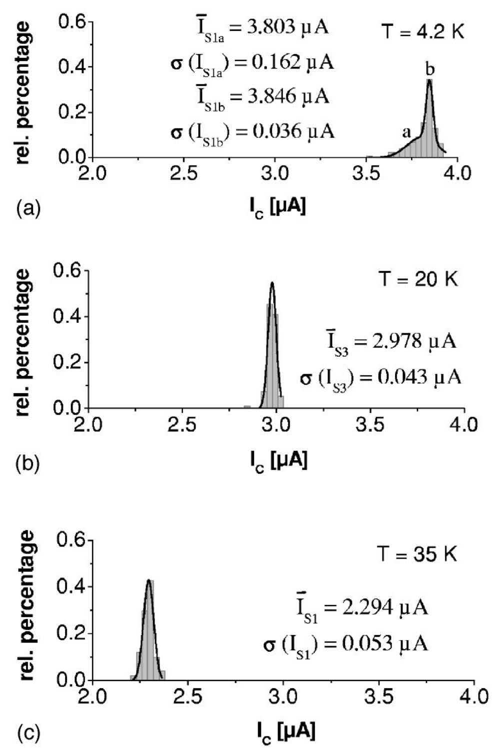

FIG. 7. The statistics of the first smallest transition current of the constricted microbridge at 4.2 K (a), 20.0 K (b), and 35.0 K (c).

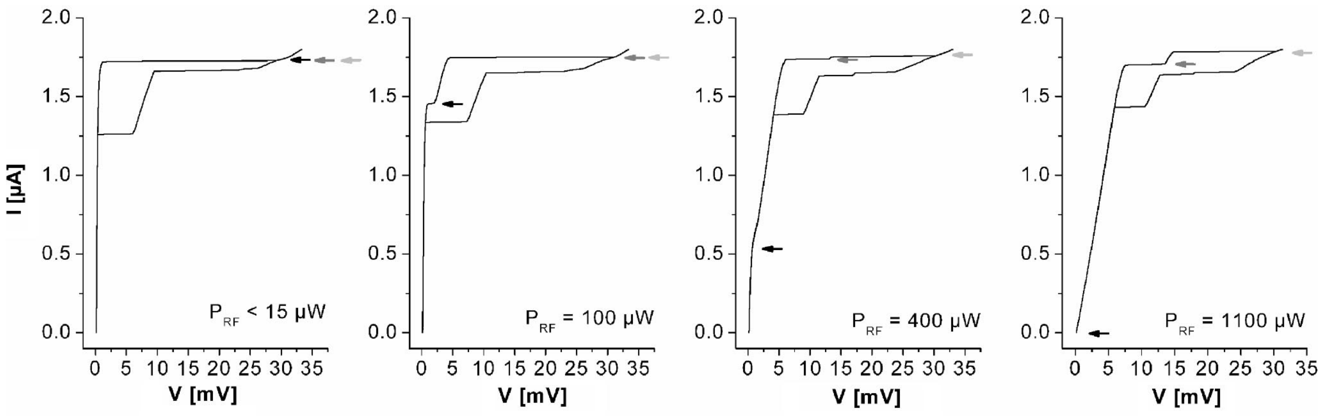

FIG. 8. IV characteristics of the constricted microbridge at 50 K for different mm-wave irradiation power with the frequency of 93 GHz.

mode configurations and by a phase locking between the Josephson junctions. Warburton *et al.* argues in the same way. Mros *et al.* also measured two several branch configurations in the IV characteristics. However, due to an increment of the operating temperature up to 60 K the 10 collective switching Josephson junctions do not split their collective behavior in our case. This fact and the small width of the bridge in the area of these switching junctions exclude the explanation approach of Mros *et al.* The approach of Machida *et al.*[24] or of Ryndyk[25] may explain the dynamics in a better way. Machida *et al.*[24] assumed an incomplete screening of the electric field of the superconducting CuO planes which leads to an interaction of the adjacent Josephson junctions and hence to a possible collective behavior. Ryndyk[25] approached the problem of the collective dynamics in intrinsic Josephson stacks by considering the quasi-neutrality breakdown effect and the quasiparticle charge imbalance effect which leads to an interaction of the junctions due to the high package density in those stacks. The case of less anisotropic stacks in Ryndyk's approach matches our situation best. These stacks show Stewart-Mc-Cumber parameters of the Josephson junctions $\beta_C = 2eI_S R_N^2 C/\hbar$, where C is the capacitance of the respective junction, between 2 and 20. This can be expected because the determination of β_C, based on the hysteresis sizes in the IV characteristics, provides values between 7 and 12.

3. Forced split ups in collective switches

The response of the constricted bridge to mm-wave irradiation (Fig. 8) is remarkable. As expected we did not find Shapiro steps because the plasma frequency $f_P = 2eI_S R_N / h\sqrt{1/2\pi\beta_C}$ of the junctions is far above the 93 GHz, but we have seen a very interesting effect: The collective switching of the 10 junctions is splitting up with increasing the AC signal amplitude gradually. As expected some junctions currents I_S get suppressed, while other parts of the junctions are still collectively switching on higher currents (see arrows in the figure). These are the junctions which contributed to the collective switch without microwave irradiation. That leads to a more multiple branch structure in the IV characteristic. We also found a splitting of the collective switching by the application of a magnetic field. However, in this case all respective transition currents are below the one without field. The reasons for these observations are unknown yet. For a theoretical approach, like the one of Ryndyk,[25] it is to notice that the mm-wave irradiation injects an additional AC quasiparticle current into the Josephson junction array. Otherwise, the assumption of Machida *et al.* in Ref. 24 should be extended to an additional fast change of the electric field with the frequency of the external irradiation over the whole stack.

C. $I_S(T)$ and $I_S(B)$

The temperature dependencies of the lowest main switching currents were taken for several bridges. All $\overline{I_S}(T)$ curves, shown in Fig. 9, run clear below the Ambegaokar-Baratoff curve which describes the expected superconductor–isolator–superconductor (SIS) junction behavior.[26] That the junction with the smallest I_S, which dominates the temperature dependence, does not show a pure tunnel behavior but likely other

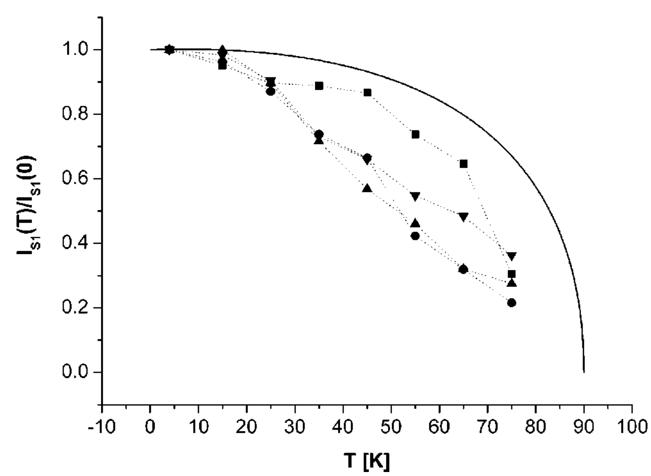

FIG. 9. The temperature dependencies of the smallest main transition current of the constricted microbridge (▼), the 2 μm wide one (▲) and two 10 μm wide ones (● and ■). The thick line represents the Ambegaokar-Baratoff fit with a reduced superconducting energy gap of $\Delta(T=0\ \text{K}) = 12$ meV.

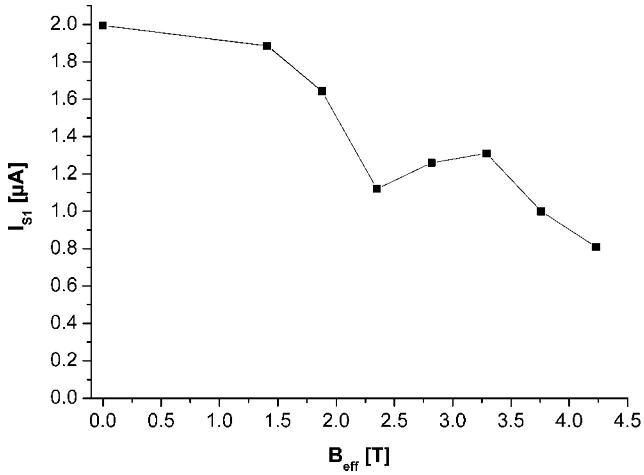

FIG. 10. The magnetic field dependence of the smallest main transition current of the constricted microbridge taken out of the respective IV characteristics measured at 50 K.

charge carriage mechanisms might be a possible explanation. The specific resistance of some 10^{-5} Ωm was calculated from the R_N values. This is not a typical value for a pure SIS tunnel junction. Another reason can be given when the different superconducting *ab*-planes are mutually tilted which leads to a not negligible tilt angle between the respective anisotropic *d*-wave orbital elements. Arie *et al.* calculated the $\overline{I_S}(T)$-behavior of ramp-edge Josephson junctions with tilted ab-plane electrodes.[27] Their calculated curves clearly show that even for large barrier parameters a tilt of the *ab*-planes leads to a $\overline{I_S}(T)$-behavior which looks like those known from superconductor–normal conductor–superconductor junctions. Remembering the film texture represented in Sec. III a tilt of the *ab*-plane is quite probable. Furthermore, we measured the magnetic field dependence of the lowest I_S of the constricted bridge at 50 K. Since there is no adjusting device we are able to measure in the effective field $B_{\text{eff}}=B\cos\phi$ which ranges from 0 to 4.7 T assuming an angle ϕ of 20° only. Figure 10 shows an I_S minimum at $B_{\text{eff}}=2.3$ T. We did not observe a complete suppression of the I_S in the given range of the magnetic field. This is the same feature as for magnetic field dependencies of mesa-shaped geometries of intrinsic Josephson junction arrays for both, thin film and single crystal based (e.g., Refs. 2 and 28–30) and as for the measurements of Chana *et al.* on similar microbridges.[15] However, note that mutual tilts in the superconducting *ab*-planes also lead to lifted minima in the $\overline{I_S}(B)$ function as it was calculated by Arie *et al.*[27]

D. Two-level fluctuations

1. General features

Time-dependent measurements on the 10 μm wide bridge reveal a two-level fluctuation (TLF) in the voltage response above the switching current which feature depends on the bias point (Fig. 11). With increasing bias current from I_S to a threshold current of about 65 μA the fluctuation launched whereas the frequency is growing with the increment of the bias. Nearby the threshold current the averaged life time of the upper and the lower level is equal. With further increment of the bias current the TLF frequency reduces again but now the upper level was preferred. At a distinct bias the TLF vanishes again. By the decrement of the bias current the same feature can be observed in the vice versa sequence. The life times at the threshold current for the upper and the lower level are several 100 μs. If the IV characteristic is driven into a larger range and driven back again, at certain current ranges multiple-level fluctuations as well as temporal turning in the level preference can be observed.

2. Cause considerations

Pesenson *et al.*[31] found intrinsic TLF in low temperature superconductor SIS tunnel junctions. Later Kemen *et al.*[32] and Herbstritt *et al.*[33] found similar intrinsic TLF in HTS grain boundary junctions. However, because in our case the microbridge consists of many serial arranged junctions a superposition of many TLF effects should be discernible. Since this is not the fact in our measurements this kind of origin can be excluded. Furthermore, TLF can also be observed due to strong quasiparticle injection.[9] Because the external quasiparticle injection into the junctions is negligible due to the sample geometry which enables superconducting feed lines to the microbridge for the bias current this explanation is improbable. The only possibility for a stronger quasiparticle injection could be given by a rather weak junction into its neighbor cluster of Josephson junction. On the other hand the TLF caused by strong quasiparticle injection did not show a turning in the level preference with changing the bias current and also no multiple-level fluctuations. A branch switching as reported in Ref. 34 can be excluded, too. In this case the TLF signals have large amplitudes (in the range of the branch distances) and appear only for bias currents nearby the branch transition. In our measurements the TLF can be observed in a wide bias current range. Jung[35] described a mechanism which led to a TLF effect in HTS layers. In such layers superconducting grains may create a superconducting loop with a grain boundary Josephson junction. These loops lead to a two level fluctuation which fits our observations. There is also a change in the level preference and an appearance and disappearance of the TLF signal due to stress changing caused by magnetic field influence or bias current. Furthermore, this explanation permits the existence of multi-level fluctuations due to several different active loops. Therefore temporal turns in the level preference can be evoked by flux jumps within the sample. Another explanation of the measured TLF effect may be given by the appearance and disappearance of vortex trains within the microbridge.[36] This would generate a phase slip in the bridge as described in Ref. 37. The features of such fluctuation signal are also indicated by level preference turning, appearance and disappearance and multiple-levels. A temporal turning in the level preference at the same bias point could possibly be due to a temporal variation of the vortex train location which leads to a changed dynamics. The probability of the existence of such loops reduces with tighter bridges in Jungs approach. Hence the TLF should vanish for a very narrow bridge. But in the case of vortex trains the

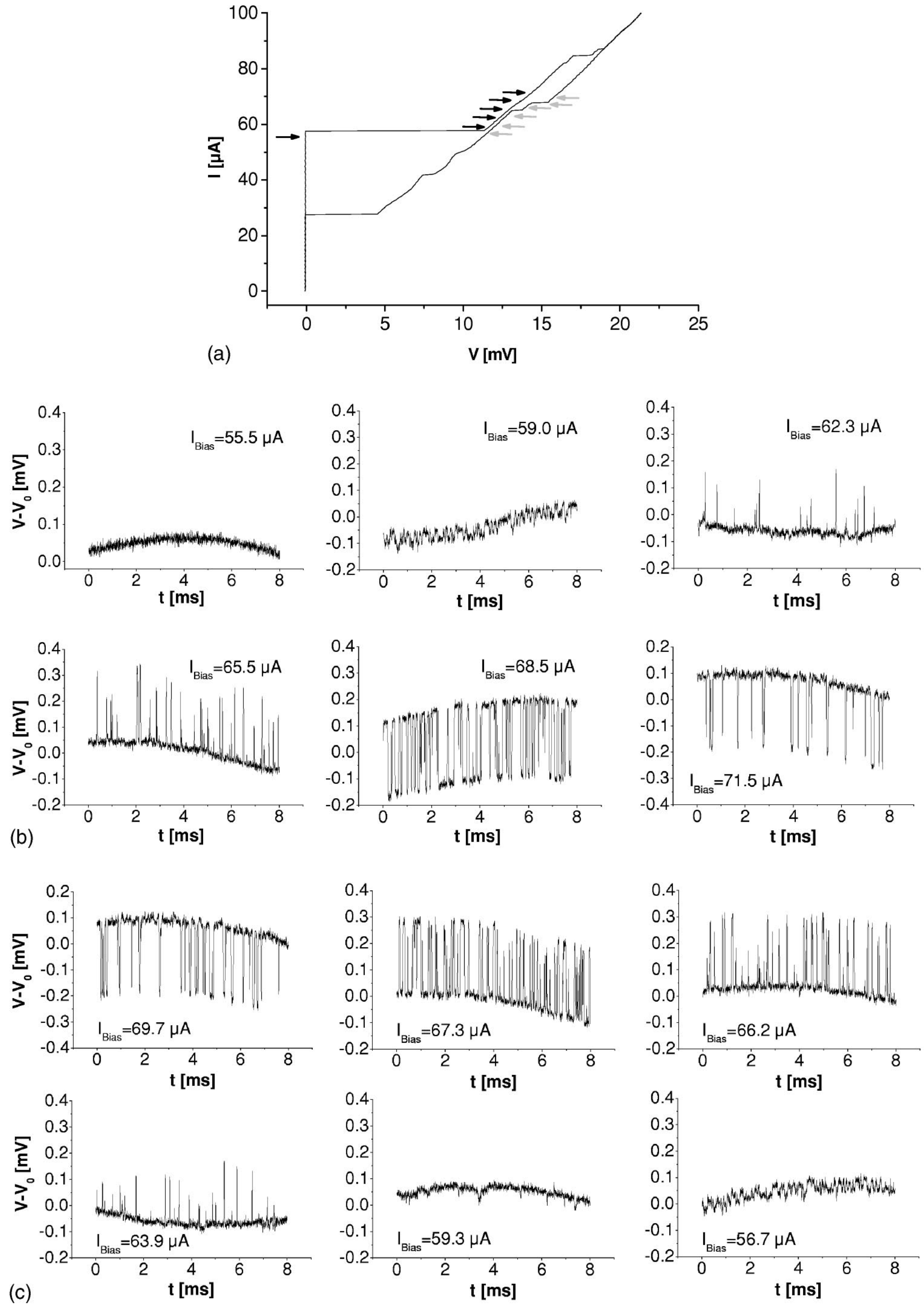

FIG. 11. (a) IV characteristic of the 10 μm wide bridge at 4.2 K. The arrows mark the constant bias points at which the respective time dependent measurements where performed (black arrows–upward; grey arrows–downward). (b) The respective time dependent measurements upwards. (c) The respective time dependent measurements downwards.

amplitude of the TLF should be larger for smaller bridges because of a stronger phase slip effect. Time dependent measurements on the constricted bridge did not show any TLF in the expected way. Additionally, the obvious grain structures in the TEM picture and the folded structures in the SEM pictures permit the imagination of the accruement of such loops as assumed by Jung.

E. Chaotic like behavior

Within the backward curve of the IV characteristics of the constricted microbridge chaotic like behavior was observable around a bias current of 2.5 μA (see Fig. 12, marked area). Time dependent measurements at this bias range show a three-level fluctuation with amplitudes of about 5 and 10 mV, respectively [Fig. 13(a)]. The amplitude values and

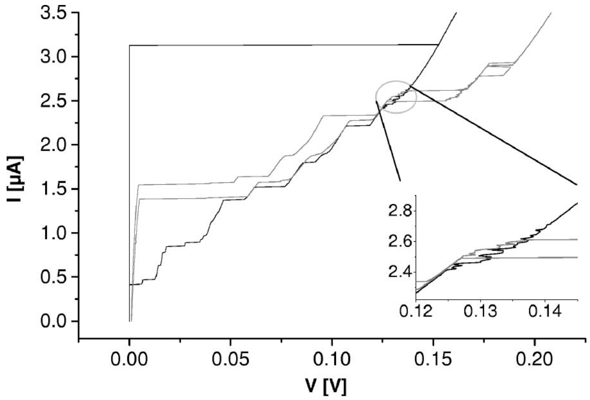

FIG. 12. IV characteristics of the constricted microbridge at 6 K without (black) and with mm-wave irradiation of a frequency of 93 GHz and a power of 30 mW (grey). The inset shows a zoomed view of the region of interest with its instability.

the features in the IV characteristics in this range enable a branch switching effect. With an irradiation of mm-wave this effect can be seen in the forward as well as in the backward part of the curves and in the same bias current range as without the irradiation again (Fig. 12) which is a remarkable fact. The time-dependent measurements with the mm-wave influence show that the amplitudes are slightly reduced and the time constants of the levels are an order of magnitude smaller than the fluctuation signal without irradiation [Fig. 13(b)]. At higher temperatures, starting at 25 K, additional chaotic like behavior appears in the IV characteristics and it increases with rising temperatures. At bias currents where the additional chaotic like behavior appears no level fluctuation in the time dependent measurements could be found and only an increased white noise is observed. This is one of the features of real chaotic behavior as it was described in Ref. 38. At temperatures higher than 45 K the chaotic behavior disappears. At 25 K a three-level fluctuation with amplitudes of about 5 and 2.5 mV is clearly recognizable in the bias range of 2.6 μA again. Now they show a dominant upper level and only short jumps into the lower and middle level. An additional mm-wave irradiation leads to the disappearance of this level fluctuation. In this case only real chaotic behavior can be seen. Due to this three-level fluctuation within a well defined bias current range we assume that its origin could be intrinsic charge trapping effects like the one reported in Ref. 39 or an interaction of instable Josephson junctions with its neighbors within a collective switching cluster.[39] Flux effects can be excluded because a thermal activation of the flux vortices should lead to a lower bias current range at which the level fluctuation appears. According to the data taken at 6 and 25 K this is not the case. The reason for the real chaotic behavior is hardly comprehensible. In Ref. 40 several possible configurations generating real chaos are mentioned: A single Josephson junction in an inductive-resistive loop, a two junction interferometer, a long single junction, a single junction under an external AC signal. In the end all these configurations represent an AC feed back to a Josephson junction which leads to the chaotic behavior for initial parameter sets. So we assume that under specific circumstances the AC feed back of the active junctions in the stack to their neighbors may lead to the observed chaos.

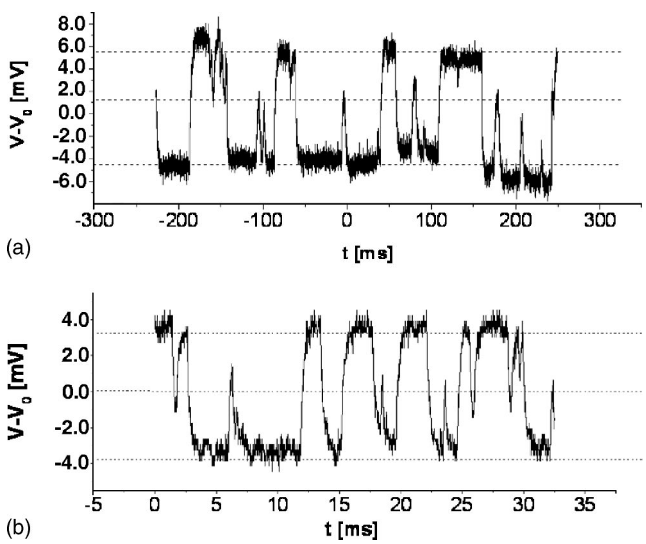

FIG. 13. The time dependent behavior of the constricted microbridge at 6 K without (a) and with the mm-wave irradiation of a frequency of 93 GHz and a power of 30 mW (b) at a constant bias current of 2.55 μA.

V. SUMMARY AND CONCLUSIONS

The microscopic investigations show that the misaligned $Tl_2Ba_2CaCu_2O_8$ films mainly grow with the given orientation of the substrate. Thin films have holes, whereas thicker films exhibit no-misaligned *c*-axis grown islands in their terrace structures. Furthermore the misaligned growth is domain-like with stacking faults in the film. Probably these domain-like film structures lead to several possible current paths in the bridges or to superconducting grains which may form superconducting loops with some intrinsic Josephson junctions. Therefore the measurements show strong statistical behavior in the IV characteristics and TLF of the wider bridges, but also slight statistical and in specific circumstances real chaotic behavior of the constricted bridge. These effects complicate the efforts for stable operation and especially for a phase synchronization of the several junctions within the microbridges. Thus, it is necessary to restrict the bridge width for a successful integration into applications. The specific resistances of the Josephson junctions exhibit that the participating barriers show a worse normal conducting behavior than a classical isolating one. This is expected to be due to the high anisotropy of the used HTS material. The reason can be assumed by dislocations and stacking faults which intrinsically shunt the barrier or form a quite weak junction itself. This and mutual tilts of the different superconducting *ab*-planes may explain the measured temperature dependence of the lowest main switching currents. A more detailed investigation of the statistical transition behavior of the constricted bridge reveals that the more junctions switch collectively the narrower is the switching current distribution. The collective switching can be split in different ways by external mm-wave irradiation as well as by magnetic field influence. However, we did not observe a splitting due to a temperature increment up to 60 K. The origin of the junction interaction within these stacks could not be clarified definitely yet. Note, that a collective switching of several junctions would support the efforts of a phase synchronization of these junctions by external feedback loops. Furthermore the chaotic like behavior found on the constricted bridge is also not clear yet. For future investigations towards any applications, an explanation of both effects the instable branch switching as well as the real chaotic behavior would be important.

ACKNOWLEDGMENTS

The authors thank A. Aßmann for the SEM and C. Voigt for the AFM inspections. This work was partially supported by the German DFG within the Contract No. Se 664/10-1 and Schn 599/2.

[1] R. Kleiner, F. Steinmeyer, G. Kunkel, and P. Muller, Phys. Rev. Lett. **68**, 2394 (1992).
[2] R. Kleiner and P. Muller, Phys. Rev. B **49**, 1327 (1994).
[3] P. Wagner, F. Hillmer, U. Frey, H. Adrian, T. Steinborn, L. Ranno, A. Elschner, I. Heyvaert, and Y. Bruynseraede, Physica C **215**, 123 (1993).
[4] F. Schmidl, A. Pfuch, H. Schneidewind, E. Heinz, L. Dörrer, A. Matthes, P. Seidel, U. Hübner, M. Veith, and E. Steinbeiss, Supercond. Sci. Technol. **8**, 740 (1995).
[5] H. Schneidewind, M. Manzel, G. Bruchlos, and K. Kirsch, Supercond. Sci. Technol. **14**, 200 (2001).
[6] S. Aukkaravittayapun, K. A. Benedict, I. G. Gorlova, P. J. King, Yu. I. Latyshev, C. Staddon, and S. G. Zybtsev, Supercond. Sci. Technol. **8**, 718 (1995).
[7] H. Imao, S. Kishida, and H. Tokutaka, Jpn. J. Appl. Phys., Part 1 **35**, 5299 (1996).
[8] L. S. Weinman, M. L. Chen, K. Viggiano, S. H. Hong, and Q. Y. Ma, IEEE Trans. Appl. Supercond. **7**, 2993 (1997).
[9] J. Scherbel, M. Mans, F. Schmidl, H. Schneidewind, and P. Seidel, Physica C **403**, 37 (2004).
[10] S. Rother, Y. Koval, P. Muller, R. Kleiner, D. A. Ryndyk, J. Keller, and C. Helm, Phys. Rev. B **67**, 024510 (2003).
[11] H. B. Wang, P. H. Wu, and T. Yamashita, Appl. Phys. Lett. **78**, 4010 (2001).
[12] S.-J. Kim and T. Yamashita, J. Appl. Phys. **89**, 7675 (2001).
[13] J. S. Tsai, J. Fujita, and M. Yu. Kupriyanov, Phys. Rev. B **51**, 16 267 (1995).
[14] O. S. Chana, A. R. Kuzhakhmetov, P. A. Warburton, D. M. C. Hyland, D. Dew-Huges, C. R. M. Grovenor, R. J. Kinsey, G. Burnell, W. E. Booij, M. G. Blamire, R. Kleiner, and P. Muller, Appl. Phys. Lett. **76**, 3603 (2000).
[15] O. S. Chana, A. R. Kuzhakhmetov, D. M. C. Hyland, D. Dew-Hughes, C. R. M. Grovenor, Y. Koval, R. Kleiner, P. Muller, and P. A. Warburton, Physica C **362**, 265 (2001).
[16] O. S. Chana, A. R. Kuzhakhmetov, D. M. C. Hyland, C. J. Eastell, D. Dew-Hughes, C. R. M. Grovenor, Y. Koval, M. Mossle, R. Kleiner, P. Muller, and P. A. Warburton, IEEE Trans. Appl. Supercond. **11**, 2711 (2001).
[17] P. A. Warburton, A. R. Kuzhakhmetov, O. S. Chana, D. M. C. Hyland, C. R. M. Grovenor, G. Burnell, M. G. Blamire, and H. Schneidewind, Physica C **372–376**, 322 (2002).
[18] A. Kawakami, Y. Uzawa, and Z. Wang, IEEE Trans. Appl. Supercond. **7**, 3126 (1997).
[19] A. Kawakami, Y. Uzawa, and Z. Wang, IEEE Trans. Appl. Supercond. **9**, 4554 (1999).
[20] G. Filatrella, N. F. Pedersen, and K. Wiesenfeld, IEEE Trans. Appl. Supercond. **11**, 1184 (2001).
[21] A. N. Grib, P. Seidel, and J. Scherbel, Phys. Rev. B **65**, 094508 (2002).
[22] A. N. Grib, J. Scherbel, and P. Seidel, Phys. Status Solidi A **198**, 142 (2003).
[23] N. Mros, V. M. Krasnov, A. Yurgens, D. Winkler, and T. Claeson, Phys. Rev. B **57**, R8135 (1998).
[24] M. Machida, T. Koyama, and M. Tachiki, Phys. Rev. Lett. **83**, 4618 (1999).
[25] D. A. Ryndyk, Phys. Rev. Lett. **80**, 3376 (1998).
[26] V. Ambegaokar and A. Baratoff, Phys. Rev. Lett. **10**, 486 (1963).
[27] H. Arie, K. Yasuda, H. Kobayashi, I. Iguchi, Y. Tanaka, and S. Kashiwaya, Phys. Rev. B **62**, 11 864 (2000).
[28] P. Seidel, F. Schmidl, A. Pfuch, H. Schneidewind, and E. Heinz, Supercond. Sci. Technol. **9**, A9 (1996).
[29] T. Yasuda, M. Tonouchi, Z. Wang, and S. Takano, Supercond. Sci. Technol. **9**, A170 (1996).
[30] A. Irie, S. Heim, S. Schromm, M. Mossle, T. Nachtrab, M. Godo, R. Kleiner, P. Muller, and G. Oya, Phys. Rev. B **62**, 6681 (2000).
[31] L. Pesenson, R. P. Robertazzi, R. A. Buhrman, S. R. Cypher, and B. D. Hunt, Phys. Rev. Lett. **67**, 2866 (1991).
[32] T. Kemen, A. Marx, L. Alff, D. Koelle, and R. Gross, IEEE Trans. Appl. Supercond. **9**, 3982 (1999).
[33] F. Herbstritt, T. Kemen, L. Alff, A. Marx, and R. Gross, Appl. Phys. Lett. **78**, 955 (2001).
[34] A. Saito, K. Hamasaki, A. Irie, and G. Oya, IEEE Trans. Appl. Supercond. **11**, 304 (2001).
[35] G. Jung, B. Savo, A. Vecchione, M. Bonaldi, and S. Vitale, Phys. Rev. B **53**, 90 (1996).
[36] S. G. Zybtsev, I. G. Gorlova, and V. Y. Pokrovskii, JETP Lett. **74**, 168 (2001).
[37] M. Tinkham, J. Low Temp. Phys. **35**, 147 (1979).
[38] R. L. Kautz, R. Monaco, J. Appl. Phys. **57**, 875 (1985).
[39] H. Matsumoto, S. Sakamoto, F. Wajima, T. Koyama, and M. Machida, Phys. Rev. B **60**, 3666 (1999).
[40] K. K. Likharev, *Dynamics of Josephson Junctions and Circuits* (Gordon and Breach, Philadelphia, 1991).